Some Properties of Molten KCl at High Density Studied by MD Simulation

Ryuzo Takagi and Isao Okada
Department of Electronic Chemistry, Tokyo Institute of Technology, Yokohama, Japan

and Kazutaka Kawamura
Research Laboratory for Nuclear Reactors, Tokyo Institute of Technology, Tokyo, Japan

Z. Naturforsch. **36a**, 1106–1111 (1981); received August 5, 1981

Molecular dynamics simulations of molten KCl have been performed at 1173 K with the molar volumes of 52.0 (the value under ambient pressure), 50.0, 48.0 and 45.0 $cm^3\ mol^{-1}$. Some thermodynamic properties at higher densities have been evaluated, which are generally in good agreement with the experimentally obtained ones and Monte Carlo results. Both at normal and higher densities, the self-exchange velocities of neighbouring unlike ions (SEV) are found to be proportional to the internal mobilities with nearly the same constant as derived previously for molten LiCl, RbCl and their 1 : 1 mixture. Calculated transport properties such as the SEV and the self-diffusion coefficients considerably decrease with increasing density, while the configuration does not change much.

Introduction

On the basis of the results of molecular dynamics simulation [1] as well as of experiments [2, 3], we have assumed that in transport phenomena of ionic melts such as diffusion and electric conduction, interactions between cation and anion and the relative volume of free space compared with the ionic size are the dominant factors. One way for elucidating the effect of the free-space on transport phenomena is to measure the properties under high pressure. Molecular dynamics simulation is a convenient tool to learn about transport properties of ionic melts under high pressure, that is at high density. Although many MD simulations have been carried out for ionic melts, only a few have been done with such a purpose.

In the present study, the self-diffusion coefficients and the self-exchange velocities of neighbouring unlike ions (SEV) of molten KCl are calculated at high density and discussed in connection with the free-space. Molten KCl was chosen, since various data of this salt are available.

MD-simulation

The pair potentials were of a Born-Mayer-Huggins type with the parameters determined for the crystal by Tosi and Fumi [4]:

$$u_{ij}(r) = z_i z_j e^2/r + A_{ij} b \exp\{(r_i^0 + r_j^0 - r)/\varrho\} - c_{ij}/r^6 - d_{ij}/r^8, \quad (1)$$

where e is the elementary charge; the parameters z, A, b, r^0, ϱ, c and d are the usually used ones in simulation of molten KCl (see, e.g. [5]). The Coulombic forces were calculated with the Ewald method [6]. The cutoff distance was $L/\sqrt{2}$ (L: the side length of the basic cell) and the vectors in the reciprocal space were counted up to $|\boldsymbol{n}|^2 = 14$. The convergence parameter was $\alpha = 4.0/L$. The step time was set as 8 fs. The number of the ions in the basic cell was 216 (108 K^+ and 108 Cl^-). The simulation was performed for the N-V-T ensemble with the method proposed by Woodcock [7]. The temperature was set as 1173 K. The molar volumes V were 52.0, 50.0, 48.0 and 45.0 $cm^3\ mol^{-1}$; these systems will be referred to as V_1, V_2, V_3 and V_4, respectively. According to the density data by Kirshenbaum et al. [8], the molar volume at 1173 K under ambient pressure is 51.96 $cm^3\ mol^{-1}$. Therefore, V_1 was regarded as of the "normal" density. The volume of 45.0 $cm^3\ mol^{-1}$ corresponds to the value somewhat below which KCl exists in the solid state at 1173 K [9]. For each system the trajectories over 4000 steps following the initial 2000 steps were used for calculation of various properties.

Reprint requests to Dr. Isao Okada, Department of Electronic Chemistry, Tokyo Institute of Technology, Nagatsuta 4259, Midori-ku, Yokohama 227, Japan.

0340-4811 / 81 / 1000-1106 $ 01.00/0. — Please order a reprint rather than making your own copy.

Results and Discussion

Thermodynamic Properties

The internal energies calculated are given in Table 1. These are in good agreement with those interpolated from the Monte Carlo results [5].

The internal pressures were calculated from the internal energies U with

$$P_i = (\partial U/\partial V)_T . \tag{2}$$

The internal pressures were evaluated to be 1.13 GPa for V_1 and 0.56 GPa for V_4, which are in satisfactory agreement with the experimentally obtained ones 0.81 GPa and 0.62 GPa, respectively [10].

The pressures were calculated according to [11]

$$P = 2\varrho_0 kT + (E_C + 6E_{DD} + 8E_{DQ})/3V + (2\pi\varrho_0^2 b/3\varrho)\int_0^{r_u}\sum_i\sum_j A_{ij} g_{ij}(r) \cdot \exp\{(r_i^0 + r_j^0 - r)/\varrho\} r^3 \mathrm{d}r , \tag{3}$$

where k is the Boltzmann constant; ϱ_0 is the number density, that is $\varrho_0 = N/V$ (N: Avogadro's number); E_C, E_{DD} and E_{DQ} are the contributions to the internal energies from the Coulombic, dipole-dipole, and dipole-quadrupole terms, respectively; $g_{ij}(r)$ is the pair correlation function between species i and j.

The upper limit for the integration r_u was taken to be 0.70 nm. Since the integration term in (3) is very sensitive to the value of $g_{ij}(r)$, $g_{ij}(r)$ was calculated by differentiating the running integration numbers for a pair $i-j$ with respect to r. Smoother curves of $g_{ij}(r)$ could be derived in this way.

In Table 2, the calculated pressures are given in comparison with the experimental values by Goldmann and Tödheide [9]. The density under ambient pressure measured by them is somewhat higher than that by Kirshenbaum et al [8]. Therefore, the pressure at the molar volume of 52.0 cm^3 mol^{-1} has a negative value according to the former data, while it is nearly zero if the latter data are taken. The calculated pressures are systematically higher than the experimental ones by ca. 0.2 GPa. This difference could be considered to be satisfactorily small, if one takes it into account that the used parameters of the pair potentials have not been evaluated originally for molten salts and that the calculated pressure is composed of mainly two large value terms of opposite sign [11], as seen from Table 2.

The isothermal compressibilities $\varkappa_T$ were calculated from the definition

$$\varkappa_T = -(1/V)(\partial V/\partial P)_T . \tag{4}$$

For V_1, $\varkappa_T$ was calculated to be 3×10^{-10} Pa^{-1}, which is somewhat smaller than 4.5×10^{-10} Pa^{-1} determined by Goldmann and Tödheide [10].

Configurations

In Fig. 1 the pair correlation functions in V_1 and V_4 are compared. The positions of the first

Table 1. Internal energy. E_C: Coulombic; E_R: short range repulsive; E_{DD}: dipole-dipole dispersion; E_{DQ}: dipole-quadrupole dispersion; U: internal energy; U_{MC}: Monte Carlo [5]; U_{expt}: experimental [19].

System	V cm^3 mol^{-1}	E_C kJ mol^{-1}	E_R	E_{DD}	E_{DQ}	U	U_{MC}	U_{expt}
V_1	52.0	− 720.5	97.9	− 21.7	− 3.3	− 618.4	− 619.9	− 614.5
V_2	50.0	− 724.7	100.6	− 22.5	− 3.4	− 620.7	− 621.7	—
V_3	48.0	− 729.0	104.5	− 23.5	− 3.5	− 622.2	− 623.2	—
V_4	45.0	− 737.0	112.5	− 25.4	− 3.8	− 624.4	—	—

Table 2. Pressure. As for the suffixes for P, see the footnote of Table 1. P_K: kinetic. $P = P_C + P_R + P_{DD} + P_{DQ} + P_K$; as for P_{exp}, see also the text.

System	P_C 10^8 Pa	P_R	P_{DD}	P_{DQ}	P_K	P	P_{expt}
V_1	− 46.22	54.13	− 8.35	− 1.68	3.75	1.63	~ 0 [8], − 0.24 [9]
V_2	− 48.31	57.90	− 9.00	− 1.81	3.90	2.68	0.67 [9]
V_3	− 50.62	62.65	− 9.78	− 1.96	4.06	4.35	2.05 [9]
V_4	− 54.60	71.83	− 11.28	− 2.30	4.34	7.99	5.37 [9]

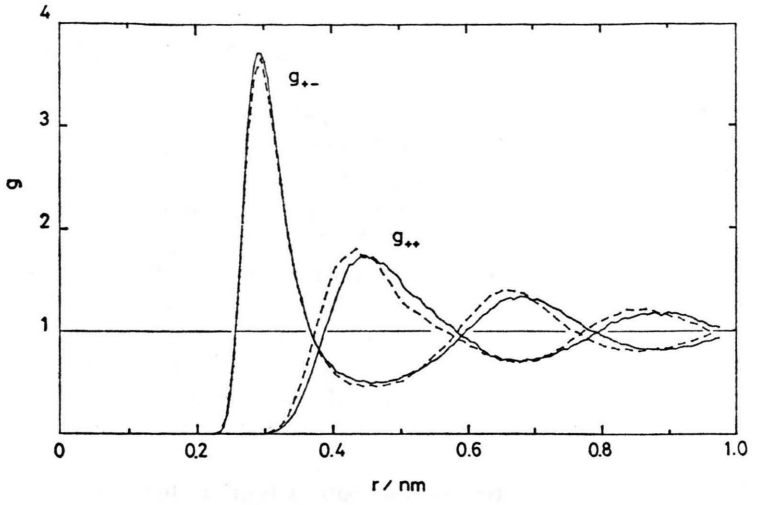

Fig. 1. Pair correlation functions. ———: V_1, – – – –: V_4.

peaks of g_{+-} and the peak heights are much the same in all the systems from V_1 to V_4 (the peak position: 0.295 nm). This trend agrees with that of the Monte Carlo results by Adams [12] in the comparable density range. The distance R_2 where g_{+-} crosses unity for the second time can be regarded as the end of the nearest neighbour interactions [13]. This is 0.365 nm irrespective of the density in the present systems. The numbers of unlike ions within R_2 around each ion are 3.7, 3.9, 4.0 and 4.3 in V_1, V_2, V_3 and V_4, respectively. The shapes of g_{++} and g_{--} are nearly identical in all the systems. The first peaks of g_{++} and g_{--} shift from 0.450 to 0.430 nm in going from V_1 to V_4.

Angular distribution functions $a_{+-+}(\theta)$ and $a_{-+-}(\theta)$, defined in a similar way as in [14], are shown in Figure 2. The distances of the two counterions from the central ion are in a range up to R_2, and the functions are normalized according to $\int_0^\pi a(\theta)\mathrm{d}\theta = 1$. The first peaks of both a_{+-+} and a_{-+-} are located around 90° in V_1 and shift towards 85° in going to V_4. The second peaks are located around 170° in all the cases and the intensity slightly increases with decreasing molar volume. Although these facts appear to suggest the presence of a distorted NaCl-type crystalline structure [15], this is not the case, as pointed out by Schäfer and Klemm [16]. The stereoscopic views depicted in Fig. 3 do not show indications of a distorted NaCl-type crystalline micro-structure. The change of the angular correlation accompanied with a decrease of molar volume seems to be larger in a_{-+-} than in a_{+-+}. This may be described to the fact that the repulsive force in the used pair potential is slightly softer for Cl-Cl than for K-K.

Thus, as far as the short range configuration is concerned, it does not change much in going from V_1 (normal density) to V_4 (high density).

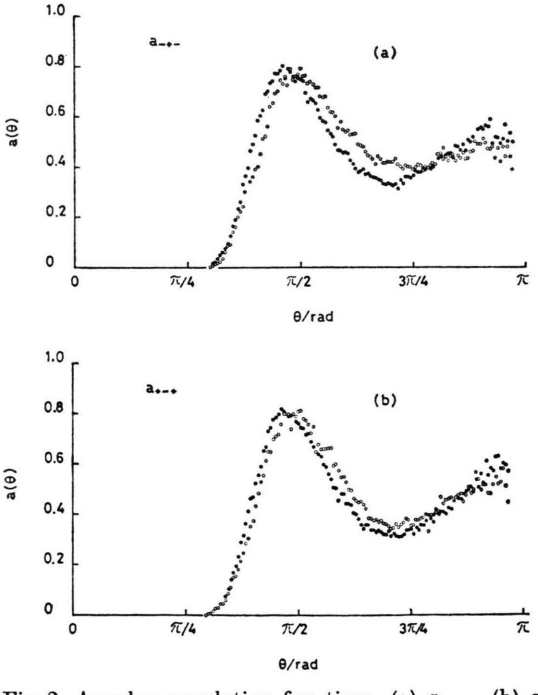

Fig. 2. Angular correlation functions. (a) a_{-+-}, (b) a_{+-+}; ○: V_1, ●: V_4.

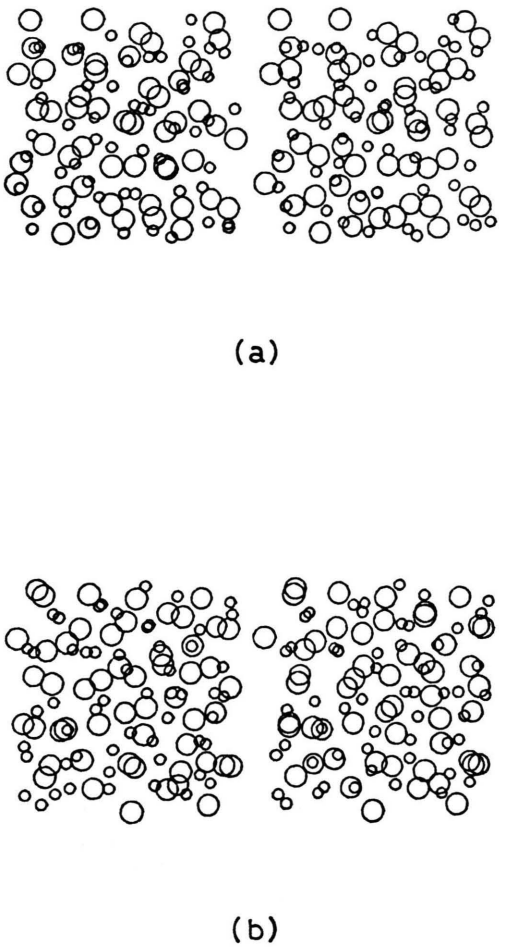

Fig. 3. Stereoscopic views. (a) V_1, (b) V_4; the relative sizes of the ions as compared with the distance between ions are represented so as to be much smaller than in reality.

Transport Properties

The self-diffusion coefficients were calculated with the Einstein equation from the mean square displacements up to 6.4 ps of totally 6480 particles for each ion. The experimental self-diffusion coefficients at 1173 K under ambient pressure [17] are also given in Table 3; they are about 0.9 times the calculated ones. The agreement could be considered to be very good. The calculated self-diffusion coefficients become smaller with a decrease of molar volume, that is of free-space volume. This trend is as expected.

The velocity autocorrelation functions (VACF) and the power spectra are shown in Figure 4. The latter are the Fourier transform of the former, the cutoff time being 0.9 ps. As the density increases, the depth of the first minimum of the VACF becomes deeper and the VACF damps more slowly. This would indicate that the average life time of the "cage" formed by the counter ions, in which the ions in question oscillate, becomes longer with decreasing molar volume.

Table 3. Self-diffusion coefficients and self-exchange velocities of neighbouring unlike ions. The values in parentheses are the experimental ones [17].

System	D_+	D_-	v
	10^{-9} m^2 s^{-1}		m s^{-1}
V_1	1.09 (0.94)	0.93 (0.84)	105
V_2	0.76	0.72	99
V_3	0.52	0.68	86
V_4	0.46	0.53	82

In Fig. 5, the SEV's are plotted against the internal mobilities, together with those calculated for other salts in the previous study [1]. The SEV, v, is defined as [1]

$$v = (R_2 - \bar{R})/\tau, \tag{5}$$

where $\bar{R}$ is the average distance of unlike ions within distance R_2, and τ the average time in which the average distance of these ions becomes R_2. The internal mobilities under high pressure in Fig. 5 are evaluated from the activation volume ΔV_Λ for the molar conductivity of molten KCl measured by Cleaver et al. [18]. Figure 5 shows that there exists a nearly linear relation between the SEV's and the internal mobilities also in the present case.

If there is an approximately linear relation between them, it follows that

$$\begin{aligned} \Delta V_\Lambda &= -RT(\partial \ln \Lambda/\partial P)_T \\ &= -RT(\partial \ln b_i/\partial P)_T \\ &\cong -RT(\partial \ln v/\partial P)_T, \end{aligned} \tag{6}$$

where Λ is the molar conductivity, b_i the internal mobility and R the gas constant. The activation volume of the SEV was calculated to be 4 cm^3 mol^{-1}, which is in fair agreement with that of the molar conductivity 6 cm^3 mol^{-1}.

In the present case the SEV decreases with decreasing free space. Meanwhile, in the MD simulation of a mixture of molten (Li-Rb)Cl, the SEV of Li^+ ions markedly increases and that of Rb^+ ions appreciably increases with a rise of LiCl concentration, that is, with a decrease of free space [1]. Al-

though these increases could not be wholly attributed to the decrease of free space, the increase of the internal mobility of Li^+ ions at least could be attributed to the decrease of the free space. Since at higher density, however, the SEV of Li^+ is expected to decrease with increasing density, there must exist an optimal volume of free space for the SEV. This value would depend on pair potentials implicitly including the concept of ionic size, moveability of coions, and temperature; this would be different from that for the self-diffusion. The existence of such an optimal volume has been suggested also for the internal mobilities from the experimental results of molten alkali nitrate mixtures [3]. For pure KCl in the present case, where the sizes of both ions are rather large, in other words, the attraction between cation and anion is not so strong, the optimal molar volume is expected to be larger than that at normal density, and hence the SEV decreases at higher density.

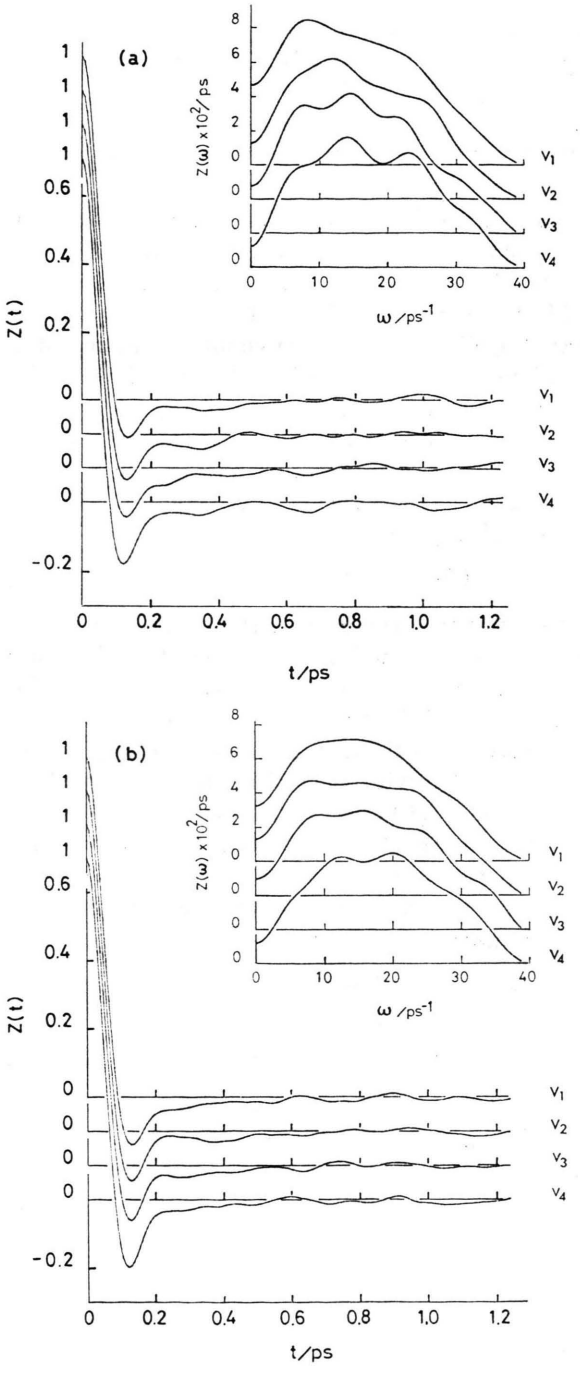

Fig. 4. Velocity autocorrelation functions $Z(t)$. The inset provides the power spectra $Z(\omega)$. (a) K^+ ion, (b) Cl^- ion.

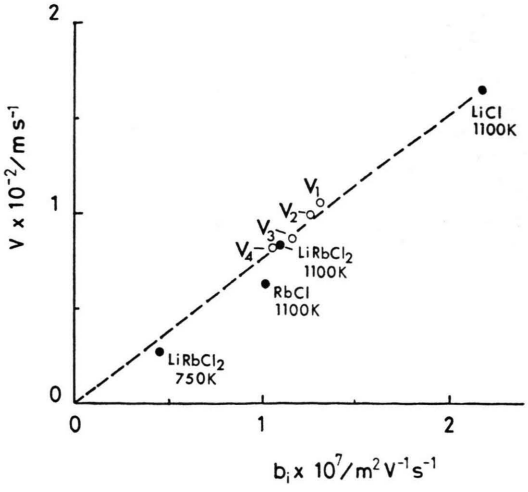

Fig. 5. Self-exchange velocities vs. internal mobilities. Open circles: this study. The solid circles were previously obtained [1]. The broken line is tentatively drawn between the circle for LiCl and the origin.

In conclusion, although in the present case the configuration is not very sensitive to a moderate decrease in molar volume, the SEV and the self-diffusion coefficients considerably decrease. This confirms that the relative volume of free space between ions plays one of the dominant roles in electric conductivity of ionic melts.

The computers HITAC M-180 and M-200 H at the Institute for Molecular Science were employed. The facilities and computer time made available to us are gratefully acknowledged.

[1] I. Okada, R. Takagi, and K. Kawamura, Z. Naturforsch. **35a**, 493 (1980).
[2] I. Okada, R. Takagi, and K. Kawamura, Z. Naturforsch. **34a**, 498 (1979).
[3] C. Yang, R. Takagi, and I. Okada, Z. Naturforsch. **35a**, 1186 (1980).
[4] M. P. Tosi and F. G. Fumi, J. Phys. Chem. Solids **25**, 45 (1964).
[5] L. V. Woodcock and K. Singer, Trans. Faraday Soc. **67**, 12 (1971).
[6] P. P. Ewald, Ann. Phys. **64**, 253 (1921).
[7] L. V. Woodcock, Chem. Phys. Lett. **10**, 257 (1971).
[8] A. D. Kirshenbaum, J. A. Cahill, P. J. McGonigal, and A. V. Grosse, J. Inorg. Nucl. Chem. **24**, 1287 (1962).
[9] G. Goldmann and K. Tödheide, Z. Naturforsch. **31a**, 656 (1976).
[10] G. Goldmann and K. Tödheide, Z. Naturforsch. **31a**, 769 (1976).
[11] L. Schäfer and A. Klemm, Z. Naturforsch. **31a**, 1068 (1976).
[12] D. J. Adams, J. Chem. Soc. Faraday Trans. II, **72**, 1372 (1976).
[13] G. Pálinkás, W. O. Riede, and K. Heinzinger, Z. Naturforsch. **32a**, 1173 (1977).
[14] B. Larsen, T. Førland, and K. Singer, Mol. Phys. **26**, 1521 (1973).
[15] B. Steffen, R. Hosemann, K. Heinzinger, and L. Schäfer, Z. Naturforsch. **32a**, 1426 (1977).
[16] L. Schäfer and A. Klemm, Z. Naturforsch. **34a**, 993 (1979).
[17] J. O'M. Bockris, S. Nanis, and N. E. Richards, J. Phys. Chem. **69**, 1627 (1965).
[18] B. Cleaver, S. I. Smedley, and P. N. Spencer, J. Chem. Soc. Faraday Trans. I, **68**, 1721 (1972).
[19] K. K. Kelley, Bull. U.S. Bur. Mines **1960**, 584.